Reduction of (pddi)Cr reveals redox noninnocence via C-C bond formation amidst competing electrophilicity: $[(cpta)CrMe_n]^-$ (n = 0, 1) and $[(pta)Cr]^-$

Alexander A. D'Arpino, Peter T. Wolczanski*, Samantha N. MacMillan,[a] Thomas R. Cundari,[b] and Mihail R. Krumov[a]

[a] A. A. D'Arpino, Prof. P. T. Wolczanski, Dr. S. N. MacMillan, Mihail R. Krumov
Department of Chemistry and Chemical Biology
Baker Laboratory, Cornell University
Ithaca, NY, USA 14853
E-mail: ptw2@cornell.edu

[b] Prof. T. R. Cundari
Department of Chemistry, CasCam
University of North Texas
Denton, TX, USA 76201

Supporting Information

Table of Contents **p**

I. Experimental

A. General Experimental. All manipulations were performed using either glovebox or high vacuum line techniques. All glassware was oven-dried for 30 min and evacuated while hot in either a glovebox chamber or on a high vacuum line. THF and diethyl ether were distilled under nitrogen from purple sodium benzophenone ketyl and vacuum transferred from the same prior to use. Hydrocarbon solvents were treated in the same manner with the addition of 1-2 mL/L tetraglyme. Benzene-d_6 was dried over sodium, vacuum transferred and stored over activated 4Å molecular sieves. THF-d_8 was dried over sodium and stored over purple sodium benzophenone ketyl.

Diimine [$Me_2C\{CH=N(1,2\text{-}C_6H_4)NH(2,6\text{-}^iPr_2C_6H_3)_2\}_2$], i.e. (pddi)$H_2$, and (pddi)Cr (**1**, CCDC-2258804) were prepared as reported.[1]

NMR spectra were acquired using Mercury 300 MHz or Bruker AV III HD 500 MHz (equipped with a 5 mm BBO Prodigy cryoprobe) spectrometers. Chemical shifts are reported relative to benzene-d_6 (^{1}H δ 7.16; $^{13}C\{^1H\}$ δ 128.06) or THF-d_8 (^{1}H δ 3.58; $^{13}C\{^1H\}$ δ 67.57). Solution magnetic measurements were conducted via Evans' method[2] in the same solvent as the ^{1}H NMR was conducted.

B. Procedures. 1. {[(cpta)Cr][K(THF)$_2$]}$_6$ (2h). To a 25 mL flask charged with (pddi)Cr (**1**, 0.163 g, 0.250 mmol) and KC_8 (0.039 g, 0.289 mmol) was added 12 mL of THF at -78 °C. The solution was slowly warmed to 23 °C and stirred for 16 h. The solution was filtered and the filtrate was triturated with Et_2O. The resulting solid was dissolved in Et_2O, concentrated to ~5 mL, and 10 mL of hexanes were added at -78 °C. After stirring for 20 min at -78 °C, the solution was cold filtered, yielding a green powder (0.113 g, 0.136 mmol, 54%). Crystals of **2h** suitable for x-ray diffraction were grown by hexane diffusion into a concentrated THF solution. ^{1}H NMR (THF-d_8): δ -39.66 ($\nu_{1/2}$ = 150 Hz), 1.29 ($\nu_{1/2}$ = 4 Hz), 3.40 ($\nu_{1/2}$ = 4 Hz), 5.14 ($\nu_{1/2}$ = 248 Hz), 7.17 ($\nu_{1/2}$ = 24 Hz), 26.18 ($\nu_{1/2}$ = 196 Hz), 47.07 ($\nu_{1/2}$ = 7.06 Hz). μ_{eff} (Evans', THF-d_8): 3.5 μ_B.

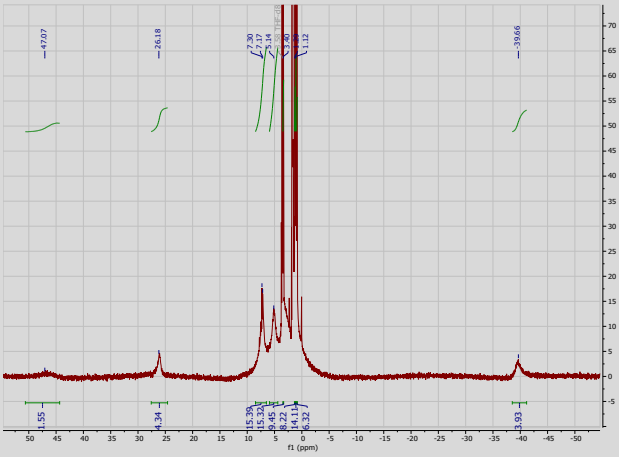

Fig S1. ^{1}H NMR spectrum of [(cpta)Cr][K(THF)$_4$] (**2**).

2. [(cpta)Cr][K(18-c-6)(THF)$_2$] (2c). To a 25 mL flask charged with (pddi)Cr (**1**, 0.509 g, 0.307 mmol), 18-crown-6 (0.212 g, 0.802 mmol), and KC_8 (0.110 g, 0.815 mmol) was added 15 mL of THF at -78 °C. The solution was slowly warmed to 23°C and stirred for 16 h. The solution was filtered and the filtrate was triturated with Et_2O. The resulting solid was dissolved in 10 mL Et_2O, concentrated to ~5 mL, and 10 mL of hexanes were added at -78 °C. After stirring for 20 min at -78 °C, the solution was cold-filtered, yielding **2c** as a green powder (0.650 g, 0.592 mmol, 76%). Crystals suitable for x-ray diffraction were grown by pentane diffusion into a concentrated THF solution. ^{1}H NMR (THF-d_8): δ -39.56 ($\nu_{1/2}$ = 280 Hz), 1.29 ($\nu_{1/2}$ = 5 Hz), 3.49 ($\nu_{1/2}$ = 36 Hz, *18-c-6*), 5.17 ($\nu_{1/2}$ = 184 Hz), 7.30 ($\nu_{1/2}$ = 4 Hz), 26.22 ($\nu_{1/2}$ = 161 Hz), 46.18 ($\nu_{1/2}$ = 6 Hz).

3. [(cpta)CrMe][Li(THF)$_4$] (3). To a 50 mL flask charged with (pddi)Cr (**1**, 0.400 g, 0.619 mmol) was added 25 mL of THF at -78 °C. A 1.6 M MeLi solution in Et_2O (0.4 mL, 0.64 mmol) was added dropwise at -78 °C with vigorous stirring. The solution was slowly warmed to 23 °C and stirred for 16 h. After removal of the volatiles, the residue was triturated with Et_2O. The resulting solid was dissolved in 15 mL Et_2O, concentrated to ~10 mL, and cooled to -78 °C. 20 mL of hexanes were added at -78 °C, and the solution was cold-filtered, yielding **3** as a green powder (0.361 g, 0.376 mmol, 63%). Crystals suitable for x-ray diffraction were grown by Et_2O diffusion into a concentrated THF solution. ^{1}H NMR (THF-d_8): δ -28.41 ($\nu_{1/2}$ = 5 Hz), 0.89 ($\nu_{1/2}$ = 6 Hz), 1.11 ($\nu_{1/2}$ = 7 Hz), 1.28 ($\nu_{1/2}$ = 6 Hz), 3.39 ($\nu_{1/2}$ = 7 Hz), 7.30 ($\nu_{1/2}$ = 7 Hz), 16.16 ($\nu_{1/2}$ = 4 Hz). μ_{eff} (Evans', THF-d_8): 2.7 μ_B.

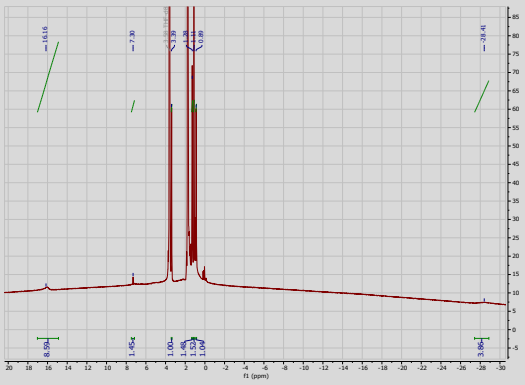

Fig S2. ^{1}H NMR spectrum of [(cpta)CrMe][Li(THF)$_4$] (**3**).

4. [(pta)Cr][Li(THF)$_4$] (4Li). To a 50 mL flask charged with (pddi)Cr (**1**, 0.506 g, 0.777 mmol) was added 25 mL of Et_2O at -78 °C. A 1.0 M $LiBEt_3H$ solution in THF (0.9 mL, 0.9 mmol) was added dropwise at -78 °C with vigorous stirring. The solution was allowed to slowly warm to 23 °C over 16 h. After removal of volatiles, the residue was triturated with Et_2O. The resulting green-brown solid was dissolved in Et_2O, concentrated to ~10 mL, cooled to -78 °C, and 20 mL of hexanes were added. The solution was cold-filtered, yielding **4Li** as a blue-green powder (0.497 g, 0.524 mmol, 68%). Crystals suitable for x-ray diffraction were grown by pentane diffusion into a concentrated THF solution. ^{1}H NMR (THF-d_8): δ 1.78 ($\nu_{1/2}$ = 12 Hz), 3.62 ($\nu_{1/2}$ = 9 Hz), 7.30 (($\nu_{1/2}$ = 8 Hz), 8.19 ($\nu_{1/2}$ = 60 Hz), 10.64 ($\nu_{1/2}$ = 218 Hz), 19.23 ($\nu_{1/2}$ = 115 Hz), 43.80 ($\nu_{1/2}$ = 668 Hz), 48.85 ($\nu_{1/2}$ = 847 Hz). μ_{eff} (Evans', THF-d_8): 3.9 μ_B.

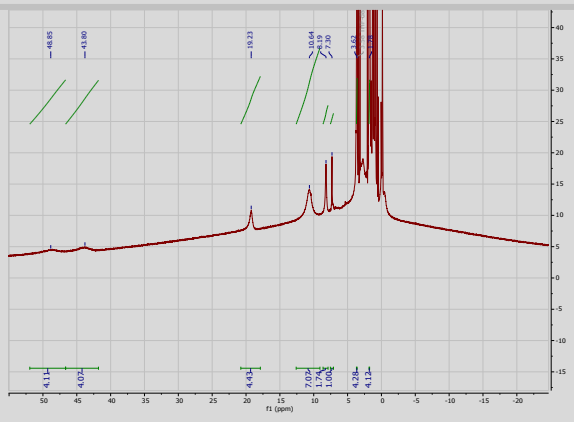

Fig S3. ^{1}H NMR spectrum of [(pta)Cr][M(THF)$_4$] (**4Li**).

5. [(pta)Cr][Na(THF)$_4$] (4Na). To a 25 mL flask charged with (pddi)Cr (**1**, 0.207 g, 0.318 mmol) and $NaBH_4$ (0.018 g, 0.476 mmol) was added 12 mL of THF at -78 °C. The solution was slowly warmed to 23 °C and stirred for 16 h. The solution was filtered and the volatiles were removed. After trituration with Et_2O, the resulting green solid was dissolved in Et_2O, concentrated to ~5 mL, and 10 mL of hexanes were added at -78 °C. The solution was stirred for 20 min at -78 °C and then cold-filtered, yielding **4Na** as a green powder (0.099 g, 0.146 mmol, 46%). ^{1}H NMR (THF-d_8): δ 0.89 ($\nu_{1/2}$ = 5 Hz), 1.16 ($\nu_{1/2}$ = 8 Hz), 1.29 ($\nu_{1/2}$ = 8 Hz), 1.78 ($\nu_{1/2}$ = 7 Hz), 3.62 ($\nu_{1/2}$ = 7 Hz), 7.30 ($\nu_{1/2}$ = 5 Hz),10.63 ($\nu_{1/2}$ = 372 Hz), 18.97 ($\nu_{1/2}$ = 214 Hz), 43.80 ($\nu_{1/2}$ = 7 Hz), 48.21 ($\nu_{1/2}$ = 7 Hz).

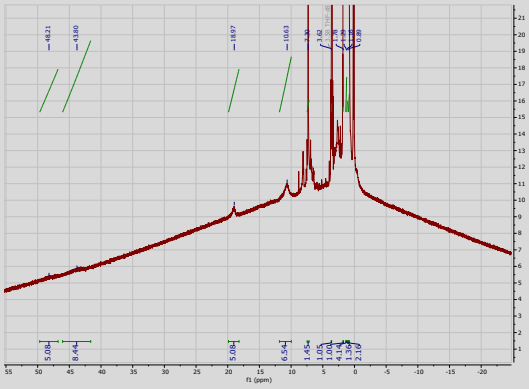

Fig S4. ^{1}H NMR spectrum of [(pta)Cr][Na(THF)$_4$] (**4Na**).

6. [(Phpta)Cr][Li(THF)$_4$] (5Ph). To a 25 mL flask charged with pddiCr (0.197 g, 0.303 mmol) was added 12 mL THF at -78 °C. 1.9 M PhLi solution in THF (0.2 mL, 0.38 mmol) was added dropwise at -78 °C with vigorous stirring. The solution was allowed to slowly warm to 23 °C while stirring for 16 h. The volatiles were removed and the residue was triturated with Et_2O. The resulting brown solid was dissolved in 15 mL Et_2O, concentrated to ~10 mL, and cooled to -78 °C. 10 mL of hexanes were added, and the solution was cold-filtered, yielding **5Ph** as an orange powder (0.165 g, 0.161 mmol, 53%). Crystals suitable for x-ray diffraction were grown by hexane diffusion into a concentrated THF solution. ^{1}H NMR (THF-d_8): δ -15.53 ($\nu_{1/2}$ = 74 Hz), -12.06 ($\nu_{1/2}$ = 419 Hz), -0.14 ($\nu_{1/2}$ =429 Hz), 6.04 ($\nu_{1/2}$ = 3619 Hz), 6.99 ($\nu_{1/2}$ = 4750 Hz), 7.30 ($\nu_{1/2}$ = 376 Hz), 9.71 ($\nu_{1/2}$ = 4382 Hz), 13.87 ($\nu_{1/2}$ = 1970 Hz).

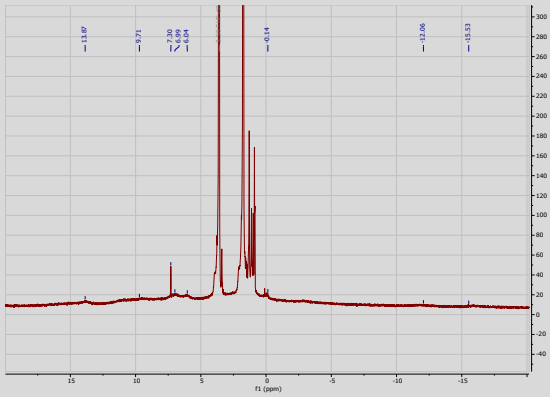

Fig S5. ^{1}H NMR spectrum of [(Phpta)Cr][Li(THF)$_4$] (**5Ph**).

7. [(bpta)Cr][K(18-c-6)(THF)$_2$] (6) and [(cpta)Cr][K(18-c-6)(THF)$_2$] (2c). To a 25 mL flask charged with (pddi)Cr (**1**, 0.107 g, 0.164 mmol), 18-crown-6 (0.054 g, 0.204 mmol), and benzyl potassium (0.023 g, 0.177 mmol) was added 15 mL of freshly distilled THF at -78 °C. The solution was slowly warmed to 23 °C and stirred for 16 h. The solution was filtered, triturated with Et_2O, dissolved in 10 mL Et_2O, and concentrated to ~5 mL. 10 mL of hexanes were added at -78 °C, and the blue-green solution was stirred for 20 min. It was cold-filtered, yielding a mixture of **2c** and **6** as a green powder (52 mg). The cocrystal of **2c:6** was grown by hexane diffusion into a concentrated THF solution. ^{1}H NMR (THF-d_8): δ -39.78 ($\nu_{1/2}$ = 302 Hz), -6.67 ($\nu_{1/2}$ = 308 Hz), 1.77 ($\nu_{1/2}$ = 5 Hz), 3.52 ($\nu_{1/2}$ = 5 Hz, 18-c-6), 3.62 ($\nu_{1/2}$ = 5 Hz), 7.14 ($\nu_{1/2}$ = 23 Hz), 7.30 ($\nu_{1/2}$ = 4 Hz), 7.32 ($\nu_{1/2}$ = 5 Hz), 14.92 ($\nu_{1/2}$ = 607 Hz), 18.53 ($\nu_{1/2}$ = 269 Hz), 26.41 ($\nu_{1/2}$ = 330 Hz), 46.19 ($\nu_{1/2}$ = 6 Hz).

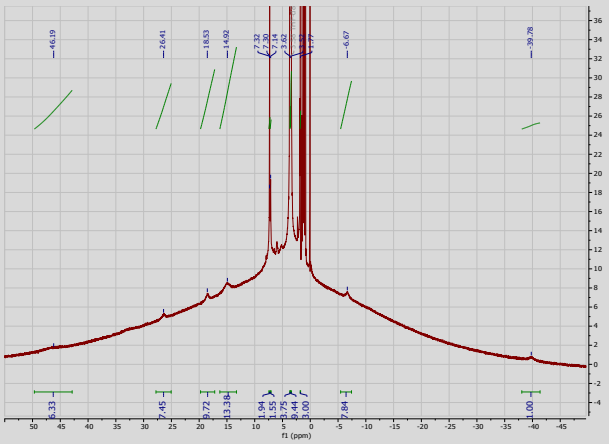

Fig S6. ^{1}H NMR spectrum of [(bpta)Cr][K(18-c-6)(THF)$_2$] (**6**) and [(cpta)Cr][K(18-c-6)(THF)$_2$] (**2c**) mixture.

8. Oxidation of [(cpta)Cr][K(THF)$_4$] (2) with [Cp$_2$Fe][PF$_6$]. To a J Young tube charged with {[(cpta)Cr][K(THF)$_2$]}$_6$ (**2h**, 22 mg, 0.026 mmol) and $FcPF_6$ (11 mg, 0.033 mmol) was added 400 µL of THF-d_8 at -78 °C. The reaction was monitored by ^{1}H NMR and after 1 d the signals of [(cpta)Cr][K(THF)$_4$] (**2**) had been replaced with those for (pddi)Cr (**1**) and Cp_2Fe (δ 4.12 ppm).

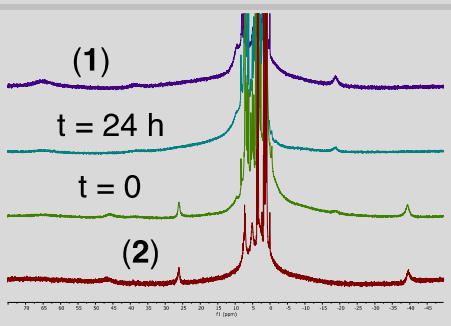

Fig S7. Oxidation of [(cpta)Cr][K(THF)$_4$] (**2**) with [Cp$_2$Fe][PF$_6$].

C. Crystallographic Data. 9. [(cpta)Cr][K(18-c-6)(THF)$_2$] (2c). Red block (0.176 x 0.14 x 0.075): $C_{61}H_{90}N_4O_8KCr$, M = 1098.46, T = 100(1) K, λ = 1.54184 Å, triclinic, P1(bar), a = 11.78630(10), b = 14.0237(2), c = 19.3145(3) Å, α = 85.0960(10)°, β = 78.0350(10)°, γ = 75.8430(10)°, V = 3026.20(7) Å^3, Z = 2, ρ (calcd) = 1.206 g/cm^3, abs. coeff. = 2.602 mm^{-1}, 73988 reflections, 13099 independent, R_{int} = 0.0390, Gaussian abs. correc., $R_1(I > 2\sigma I)$ = 0.0403, wR_2 = 0.1085, R_1(all data) = 0.0425, wR_2 = 0.1102, GOF = 1.085, CCDC-2345830.

10. {[(cpta)Cr][K(THF)$_2$]}$_6$ (2h). Brown plate (0.201 x 0.157 x 0.082): $C_{102}H_{140}N_8O_5K_2Cr_2$, M = 1740.41, T = 102.6(5) K, λ = 1.54184 Å, trigonal, R3(bar), a = b = 41.8744(3), c = 15.47760(10) Å, α = 90°, β = 90°, γ = 120°, V = 23503.4(4) Å^3, Z = 9, ρ (calcd) = 1.107 g/cm^3, abs. coeff. = 2.817 mm^{-1}, 156996 reflections, 11157 independent, R_{int} = 0.0807, Gaussian abs. correc., $R_1(I > 2\sigma I)$ = 0.0678, wR_2 = 0.2045, R_1(all data) = 0.0782, wR_2 = 0.2192, GOF = 1.047, CCDC-2345833.

11. [(cpta)CrMe][Li(THF)$_4$] (3). Green needle (0.419 x 0.084 x 0.068): $C_{62}H_{95}N_4O_5LiCr$, M = 1035.35, T = 101(1) K, λ = 1.54184 Å, triclinic, P1(bar), a = 11.76990(10), b = 16.1506(2), c = 17.7227(2) Å, α = 97.6690(10)°, β = 105.2700(10)°, γ = 108.7830(10)°, V = 2987.76(6) Å^3, Z = 2, ρ (calcd) = 1.151 g/cm^3, abs. coeff. = 1.952 mm^{-1}, 80638 reflections, 12726 independent, R_{int} = 0.0485, Gaussian abs. correc., $R_1(I > 2\sigma I)$ = 0.0465, wR_2 = 0.1275, R_1(all data) = 0.0480, wR_2 = 0.1288, GOF = 1.062, CCDC-2345831.

12. [(pta)Cr][Li(THF)$_4$] (4Li). Brown block (0.244 x 0.187 x 0.112): $C_{61}H_{92}N_4O_5LiCr$, M = 1020.32, T = 100(1) K, λ = 1.54184 Å, triclinic, P1(bar), a = 12.36550(10), b = 14.1523(2), c = 19.2237(3) Å, α = 69.5230(10)°, β = 76.2320(10)°, γ = 65.5100(10)°, V = 2850.94(7) Å^3, Z = 2, ρ (calcd) = 1.189 g/cm^3, abs. coeff. = 2.039 mm^{-1}, 66068 reflections, 12309 independent, R_{int} = 0.0609, Gaussian abs. correc., $R_1(I > 2\sigma I)$ = 0.0541, wR_2 = 0.1483, R_1(all data) = 0.0563, wR_2 = 0.1510, GOF = 1.048, CCDC-2345829.

13. [(bpta)Cr][K(18-c-6)(THF)$_2$] (6) and [(cpta)Cr][K(18-c-6)(THF)$_2$] (2c). Red block (0.277 x 0.139 x 0.111): $C_{140}H_{202}N_8O_{17}K_2Cr_2$, M = 2451.28, T = 100.2(5) K, λ = 1.54184 Å, triclinic, P1(bar), a = 12.11610(10), b = 19.5547(2), c = 29.7051(2) Å, α = 82.7670(10)°, β = 81.4080(10)°, γ = 78.7040(10)°, V = 6790.16(11) Å^3, Z = 2, ρ (calcd) = 1.199 g/cm^3, abs. coeff. = 2.376 mm^{-1}, 181578 reflections, 29216 independent, R_{int} = 0.0463, Gaussian abs. correc., $R_1(I > 2\sigma I)$ = 0.0580, wR_2 = 0.1593, R_1(all data) = 0.0614, wR_2 = 0.1623, GOF = 1.015, CCDC-2345832.

D. Electrochemical Studies. Tetrabutylammonium perchlorate (98%, TCI America) was purified by recrystallization from ethanol followed by vacuum drying at 80 °C for several days. Anhydrous and BHT-free tetrahydrofuran (99.8%, Alfa Aesar) was used as received. A glass, three-compartment electrochemical cell was dried in an oven at 100 °C overnight to remove adsorbed water prior to experiments. All electrochemical measurements were performed inside an argon filled glovebox where oxygen and water levels were kept below 1 ppm. A glassy carbon disk (3 mm diam.) sealed in Teflon was used as the working electrode and was polished with 0.05 µm alumina powder prior to experiments. The reference electrode was silver/silver nitrate separated from the bulk electrolyte by a fine glass frit. A graphite rod was used as the counter. Electrochemical measurements were performed using an electrochemical workstation (CH Instruments, model 920D). A background voltammogram was recorded in 0.2 M TBAP solution in THF to ensure no electrolyte contaminants are present. The analyte was then added to the electrolyte to obtain a 7.5 mM solution.

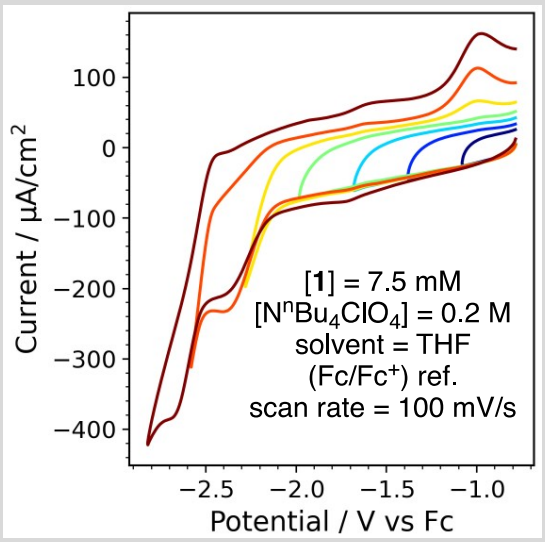

Fig. S8. Cyclic voltammograms of (pddi)Cr (**1**) showing that the appearance of $E°_{ox}$ = -2.53 V is dependent on the reduction at $E°_{red}$ = -2.76 V.

In Fig. S8, cycling after reduction at -2.50 V shows no oxidation wave until -0.99 V. As the cycling is shifted to more negative potentials the oxidation wave at -2.53 V starts to appear (brown cycle), and completely appears as shown in Fig. 5 (main text). Note that the features at high negative potentials are affected by capacitance issues that limited acquiring of data to a maximun scan rate of 100 mV/s.

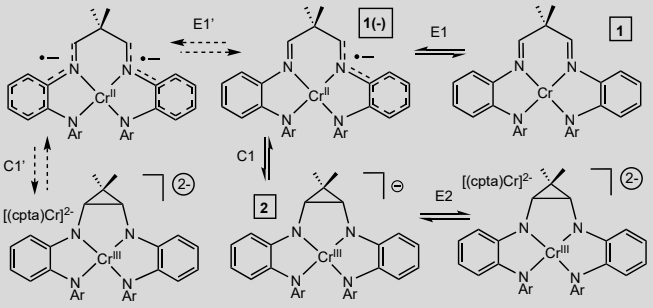

Scheme S1. Modeling scheme of reduction of (pddi)Cr (**1**) to [(cpta)Cr]$^-$ (**2**).

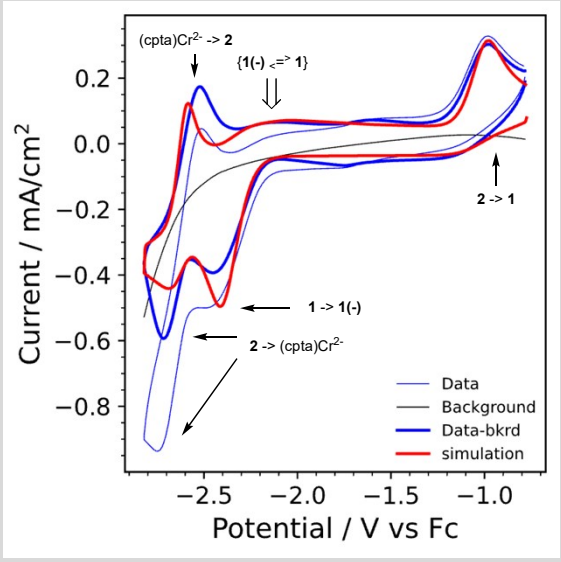

Fig S9. Simulation of (pddi)Cr (**1**) reduction of (pddi)Cr (**1**) to [(cpta)Cr]$^{-}$ (**2**).

In Fig. S9, the simulation (red line) of the CV (main text Fig. 5) is shown, and it supports the EC mechanism described in the text and in the solid line equilibria in Scheme S1. Note that background (thin line; Background) capacitance issues are likely responsible for much of the curvature. Subtraction of the background renders the redox features more regular (thick blue line; Data-bkrd), consistent with the proposed 1e^{-} redox events. Scheme S1 was used in the simulation, with E(1 forward) = 5e^{-4} cm/s and E(1 reverse) = 1e^{-3}. As long as the chemical step, i.e. C-C bond formation is >10 s^{-1}, the second reduction to (cpta)Cr^{2-} occurs via reduction of **2**. Only in the case where C1 in is slower that ~1 s^{-1} ($\Delta G^{\ddagger}$ ~ 66 kJ/mol) does an oxidation wave grow in at ~-2.2 V (E1' -C1') at the expense of the oxidation wave at -0.99 V. Efforts to obtain interpretable faster scans than 100 mV/s were unfeasible in THF at these potentials. Since C-C bond formation from reduction of **1** (**1** -> **1(-)** -> **2**) might approach vibrational unimolecular rates, the CV supports the second reduction as **2** -> (cpta)Cr^{2-}.

E. Computational Information. 1. Methods. Calculations employed the Gaussian 16 code.[3] Specifically, the M06 functional[4] was used in conjunction with the 6-31G(d) all-electron basis set for initial geometry optimizations. All simulations assumed a continuum solvent, THF, within the SMD approximation.[5] Geometry optimizations did not assume any molecular symmetry, and were conducted for all pertinent high-, intermediate- and low-spin states. Calculation of the energy Hessian was performed at all stationary points to identify the geometries as local minima or transition states. Reported free energies are for the most stable electronic ground state multiplicities. For more accurate energies, a single point calculation at the M06/6-311++G(d,p)/SMD-THF was performed, and to this electronic energy was added the enthalpic and entropic corrections (unscaled vibrational frequencies) derived from the initial M06/6-31+G(d)/SMD-THF computation.

2. Optimized Geometries. The optimized geometries for (pddi)Cr (**1**), [(cpta)Cr][K(THF)$_4$] (**2**), and [(cpta)CrMe][Li(THF)$_4$] (**3**) are given in Figures S9, S10 and S11, respectively.

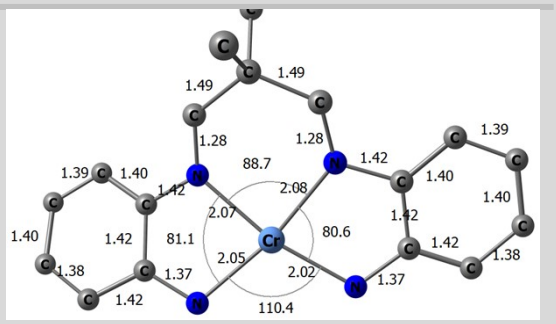

Fig S10. Core geometry for quintet (pddi)Cr (**1**).

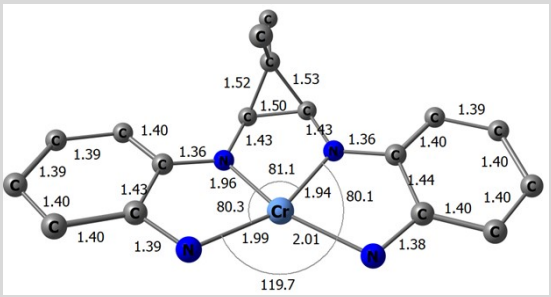

Fig S11. Core geometry for quartet [(cpta)Cr][K(THF)$_4$] (**2**).

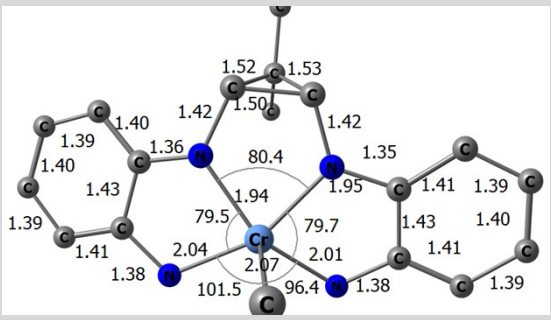

Fig S12. Core geometry for triplet [(cpta)CrMe][Li(THF)$_4$] (**3**).

3. Selected Molecular Orbitals. a. (pddi)Cr (1). Quintet; M06/6-311++G(d,p)/SMD-THF; IsoValue = 0.045 a.u.

#	e_{alpha} (eV)	Status	e_{beta}	Status
163	-7.97	Occupied	-7.89	Occupied
164	-7.76	Occupied	-7.67	Occupied
165	-6.80	Occupied	-6.74	Occupied
166	-6.76	Occupied	-6.70	Occupied
167	-6.51	Occupied	-6.50	Occupied
168	-6.30	Occupied	-6.30	Occupied
169	-6.29	Occupied	-6.12	Occupied
170	-6.18	Occupied	-6.06	Occupied
171	-6.05	Occupied	-5.09	Occupied
172	-5.93	Occupied	-5.06	Occupied
173	-5.76	Occupied	-1.35	Unoccupied
174	-5.39	Occupied	-1.15	Unoccupied
175	-4.85	Occupied	-0.64	Unoccupied
176	-4.54	Occupied	0.16	Unoccupied
177	-1.23	Unoccupied	0.35	Unoccupied
178	-1.17	Unoccupied	0.38	Unoccupied
179	0.12	Unoccupied	0.45	Unoccupied
180	0.36	Unoccupied	0.59	Unoccupied
181	0.46	Unoccupied	0.70	Unoccupied
182	0.59	Unoccupied	0.82	Unoccupied
183	0.69	Unoccupied	0.98	Unoccupied
184	0.89	Unoccupied	1.14	Unoccupied
185	1.03	Unoccupied	1.55	Unoccupied

186	1.13	Unoccupied	1.66	Unoccupied
187	1.18	Unoccupied	1.76	Unoccupied
188	1.25	Unoccupied	2.20	Unoccupied
189	1.36	Unoccupied	2.30	Unoccupied
190	1.93	Unoccupied	2.49	Unoccupied
191	2.27	Unoccupied	2.73	Unoccupied
192	2.67	Unoccupied	2.96	Unoccupied

i. **alpha orbitals.**

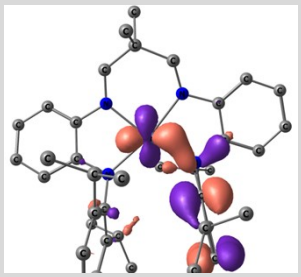

169α; Cr d(δ), Dipp(π)

170 α; Dipp(π)

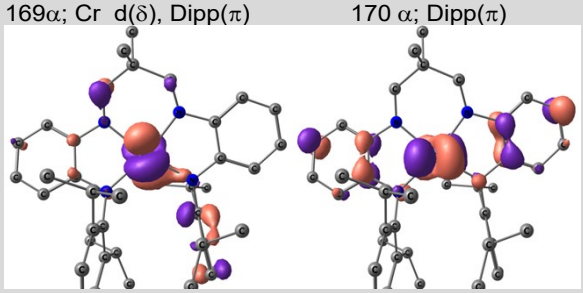

171α; Cr d(π), L(π)

172α; Cr d(π)

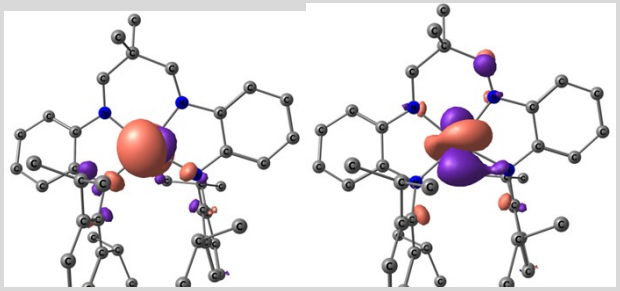

173 α; Cr d(π)

174 α; Cr d(σ)

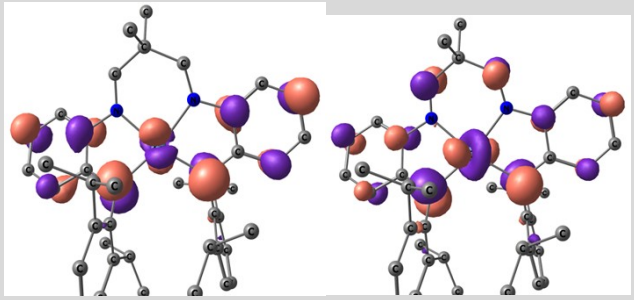

175α; L(π), some Cr d(π)

176α(HOMO); L(π), some Cr d(π)

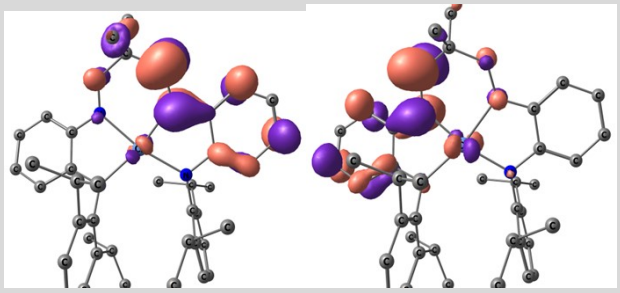

177α (LUMO); L(π*)

178α; L(π*)

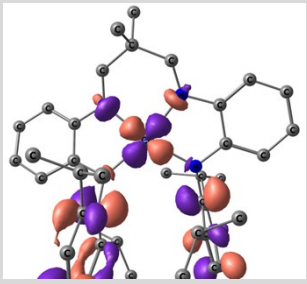

179α; Cr d(σ*), Dipp(π*)

---

ii. **beta orbitals.**

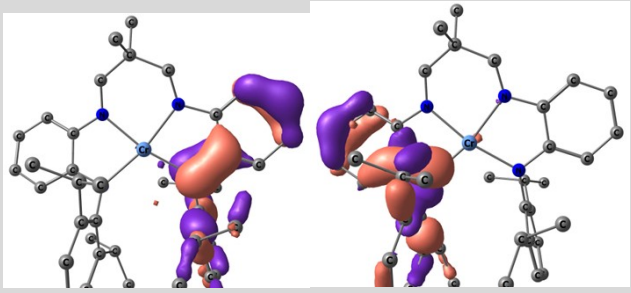

163β; L(π)

164β; L(π)

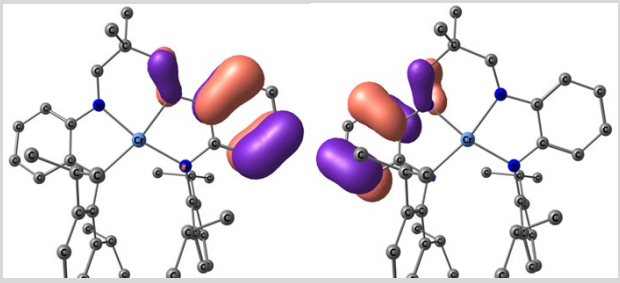

165β; L(π)

166β; L(π)

167-170 β; Dipp(π)

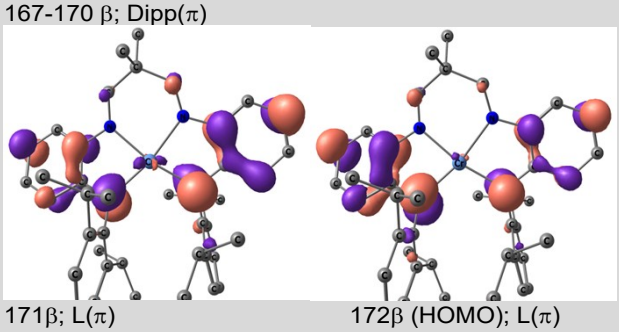

171β; L(π)

172β (HOMO); L(π)

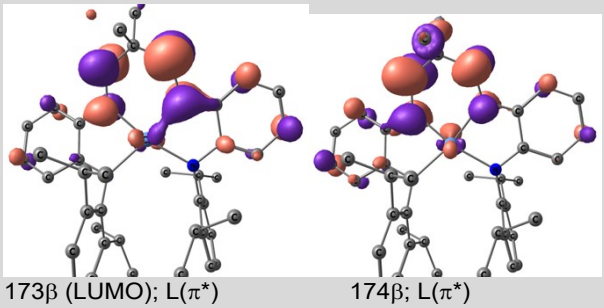

173β (LUMO); L(π*)

174β; L(π*)

175-176β; diffuse metal orbitals

177-180β; Dipp (π*)

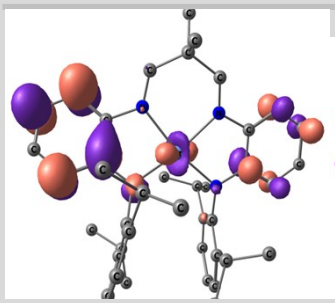
181β; L(π*)

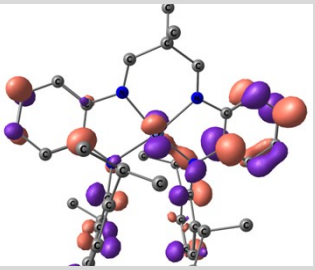
182β; L(π*), Dipp (π*)

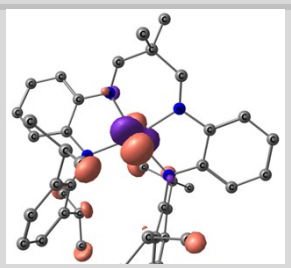
190β; Cr(d)
191β; diffuse

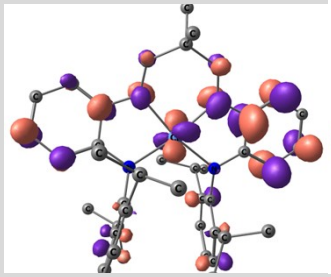
183β; L(π*)

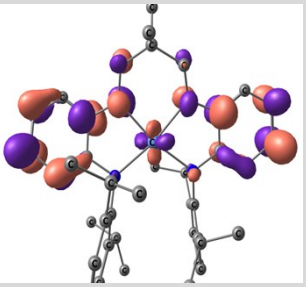
184β; L(π*)

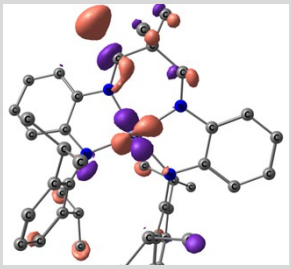
192β; Cr(d)

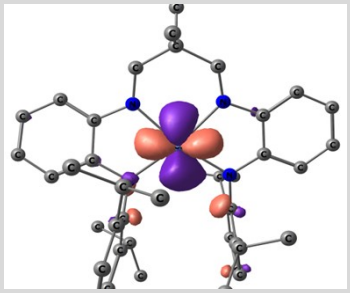
185β; Cr(d)

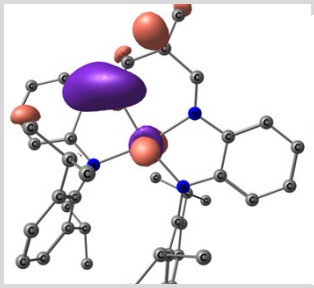
186β; diffuse orb, Cr(d)

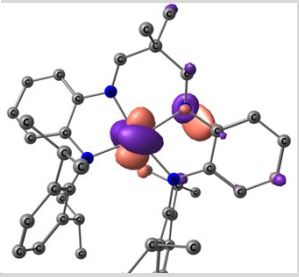
187β; Cr(d)

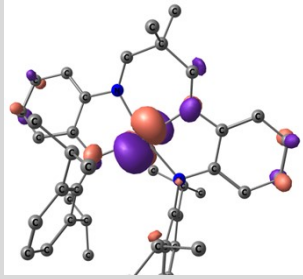
188β; Cr(d)

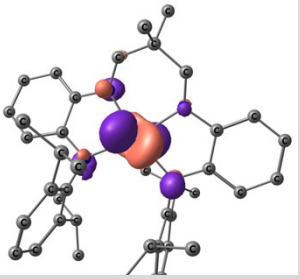
189β; Cr(d)

iii. **MO diagram.**

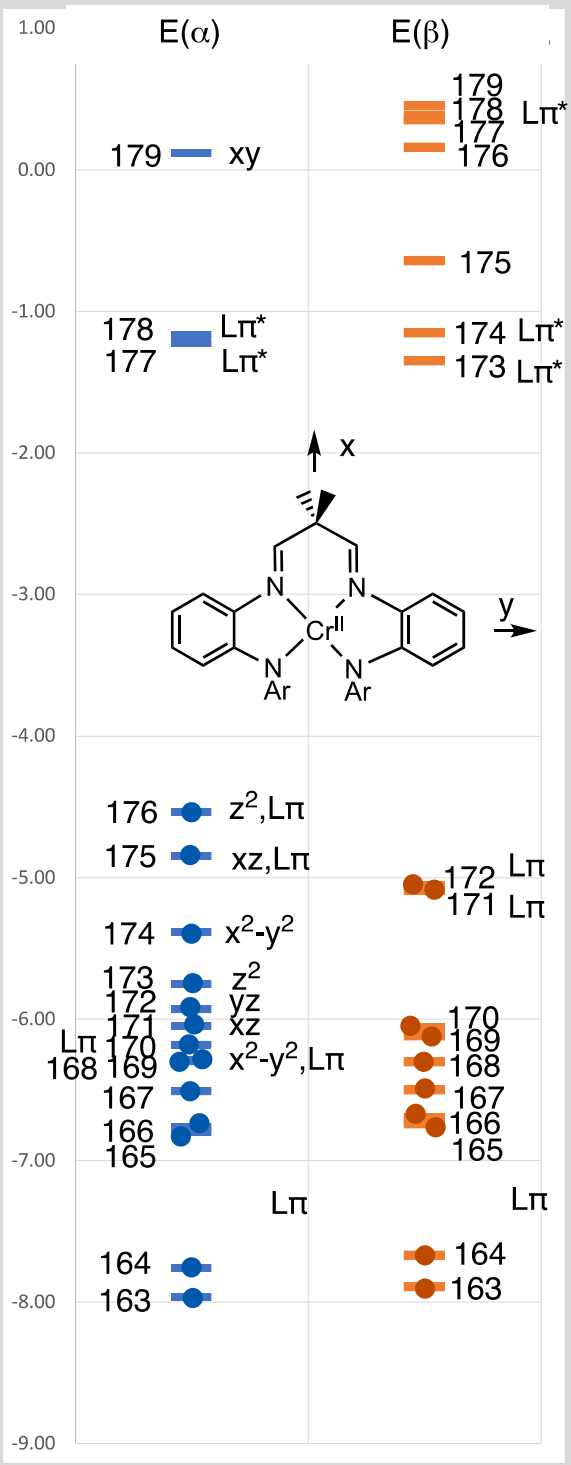

---

b. [(cpta)Cr]K (2). Quartet; M06/6-311++G(d,p)/SMD-THF; IsoValue = 0.045 a.u.

#	e_{alpha} (eV)	Status	e_{beta}	Status
170	-5.83	Occupied	-5.35	Occupied
171	-5.37	Occupied	-5.14	Occupied
172	-5.20	Occupied	-4.10	Occupied
173	-4.99	Occupied	-4.03	Occupied
174	-4.44	Occupied	0.27	Unoccupied
175	-4.36	Occupied	0.57	Unoccupied
176	-3.77	Occupied	0.70	Unoccupied
177	-1.39	Unoccupied	0.79	Unoccupied
178	0.59	Unoccupied	0.83	Unoccupied
179	0.65	Unoccupied	1.17	Unoccupied
180	0.81	Unoccupied	1.24	Unoccupied
181	0.84	Unoccupied	1.28	Unoccupied
182	1.29	Unoccupied	1.57	Unoccupied
183	1.55	Unoccupied	1.69	Unoccupied
184	1.65	Unoccupied	1.88	Unoccupied
185	1.71	Unoccupied	2.13	Unoccupied
186	1.85	Unoccupied	2.37	Unoccupied
187	1.95	Unoccupied	2.55	Unoccupied
188	2.13	Unoccupied	2.67	Unoccupied

***i.* alpha orbitals.**

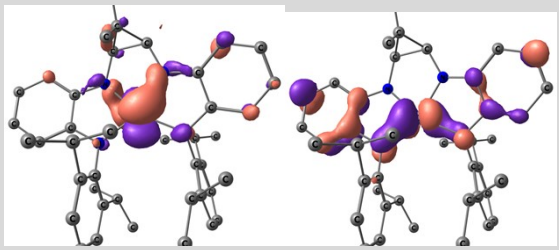
171α; Cr(dπ) 172α; Cr(dπ)

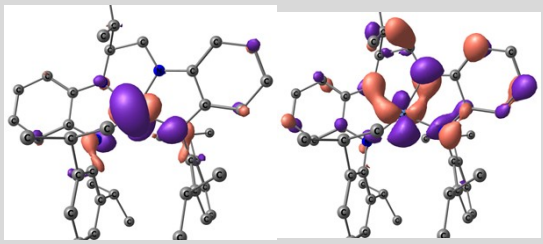
173α; Cr(dσ) 174α; Cr(dδ), L(π)

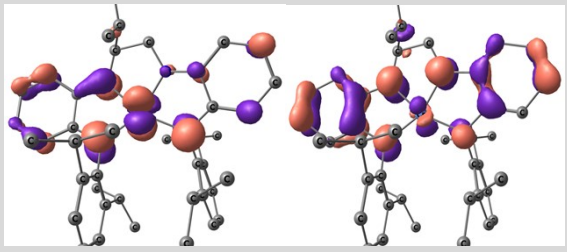
175α; Cr(dπ), L(π) 176α (HOMO); L(π)

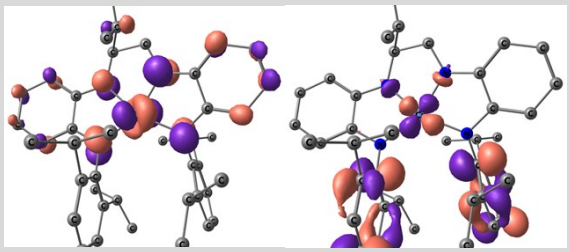
177α (LUMO): Cr(dπ), L(π*) 178α; Cr(dδ), Dipp(π*)

***ii.* beta orbitals.**

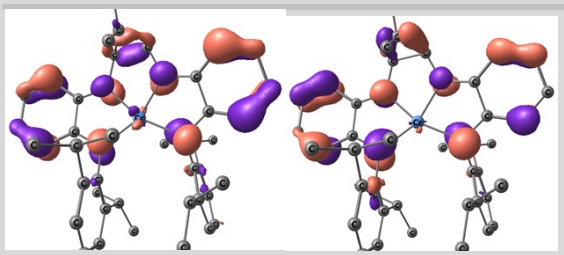

170β: L(π) 171β; L(π)

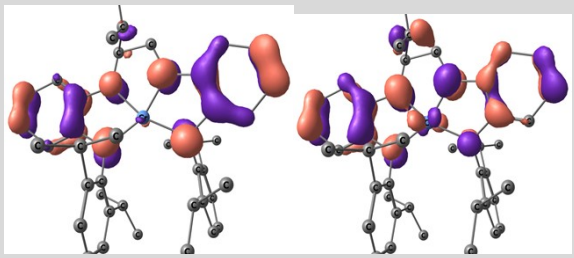

172β: L(π) 173β (HOMO); L(π)

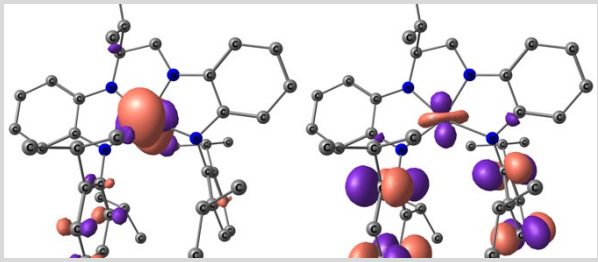

174β (LUMO); Cr (dσ) 175β; Cr (dδ*), Dipp (π*)

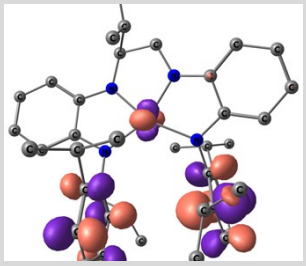

176β; Cr (dσ), Dipp (π*)
177β & 178β; Dipp (π*)

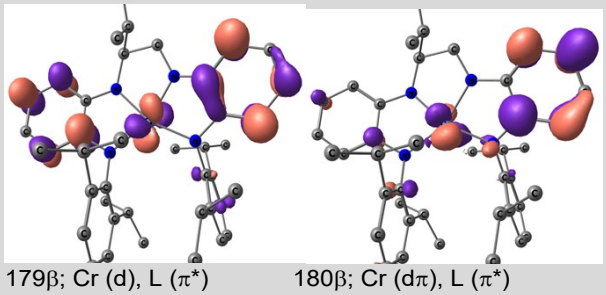

179β; Cr (d), L (π*) 180β; Cr (dπ), L (π*)

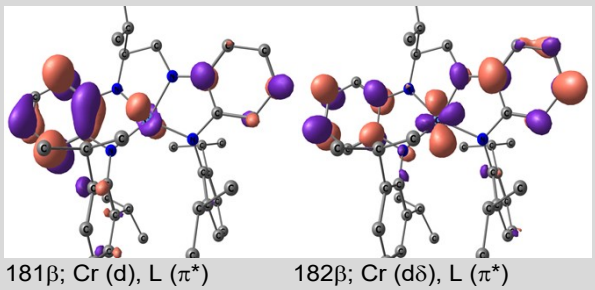

181β; Cr (d), L (π*) 182β; Cr (dδ), L (π*)
183β; diffuse

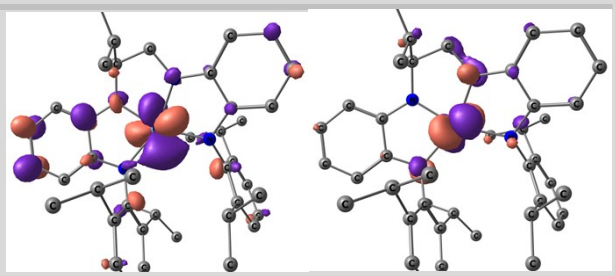

184β; Cr (dπ*), L (π*) 185β; Cr (dπ)

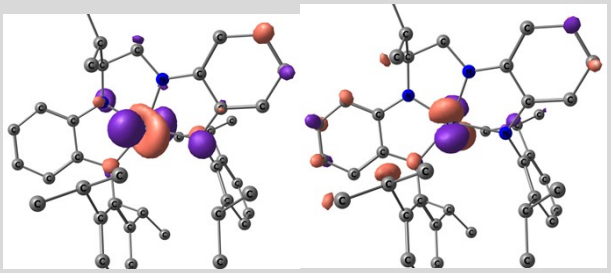

186β; Cr (d) 187β; Cr (dπ)

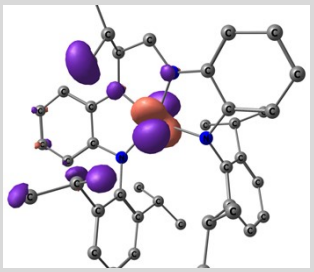

188β; Cr (d)

---

iii. **MO diagram.**

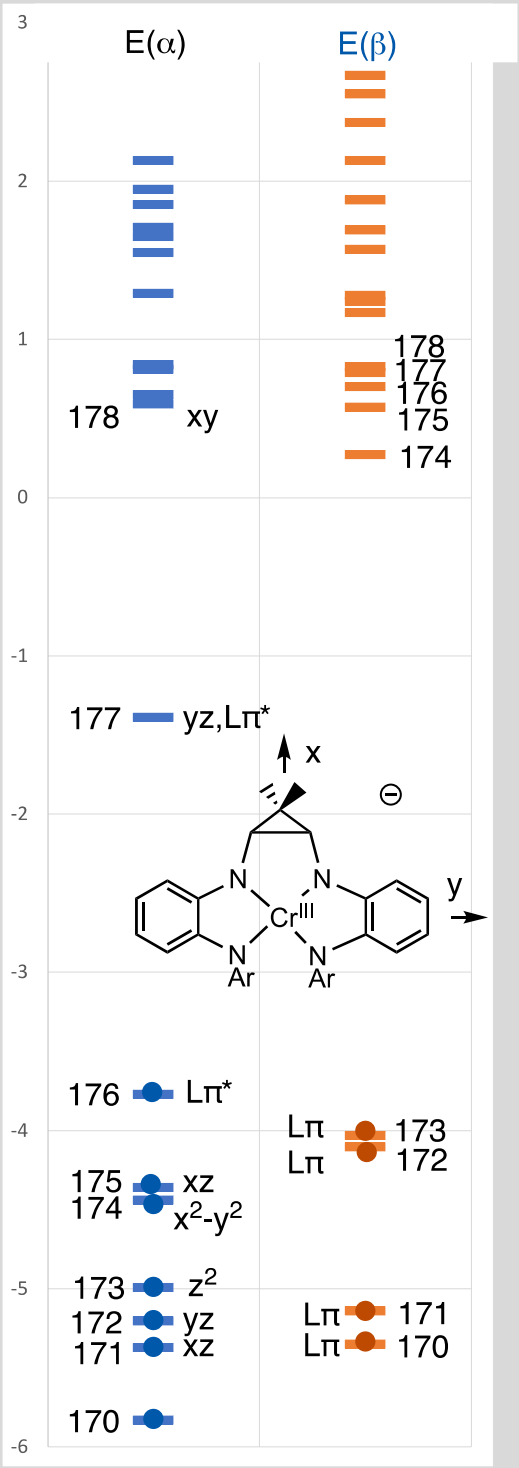

---

c. [(cpta)CrMe][Li(THF)$_4$] (3). Triplet; M06/6-311++G(d,p)/SMD-THF; IsoValue = 0.045 a.u.

#	e_{alpha} (eV)	Status	e_{beta}	Status
170	-6.47	Occupied	-6.25	Occupied
171	-6.24	Occupied	-6.04	Occupied
172	-6.11	Occupied	-6.03	Occupied
173	-6.09	Occupied	-5.99	Occupied
174	-6.02	Occupied	-5.86	Occupied
175	-5.95	Occupied	-5.42	Occupied
176	-5.35	Occupied	-5.20	Occupied
177	-5.21	Occupied	-4.19	Occupied
178	-4.83	Occupied	-4.11	Occupied
179	-4.43	Occupied	0.47	Unoccupied
180	-3.98	Occupied	0.58	Unoccupied
181	-1.71	Unoccupied	0.73	Unoccupied
182	-0.10	Unoccupied	0.81	Unoccupied
183	0.47	Unoccupied	0.91	Unoccupied
184	0.58	Unoccupied	1.04	Unoccupied
185	0.78	Unoccupied	1.12	Unoccupied
186	0.88	Unoccupied	1.35	Unoccupied
187	1.40	Unoccupied	1.59	Unoccupied
188	1.46	Unoccupied	1.61	Unoccupied
189	1.58	Unoccupied	1.84	Unoccupied
190	1.66	Unoccupied	1.94	Unoccupied
191	1.73	Unoccupied	2.21	Unoccupied
192	1.91	Unoccupied	2.57	Unoccupied
193	1.98	Unoccupied	2.63	Unoccupied
194	2.62	Unoccupied	2.75	Unoccupied
195	2.67	Unoccupied	3.23	Unoccupied
196	3.13	Unoccupied	3.28	Unoccupied

***i.* alpha orbitals.**

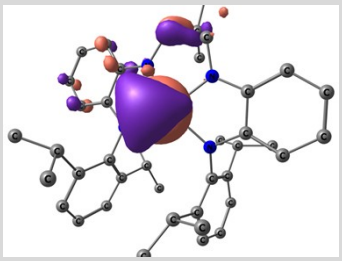

170α; CrMe (σ)
171α; Dipp (π)

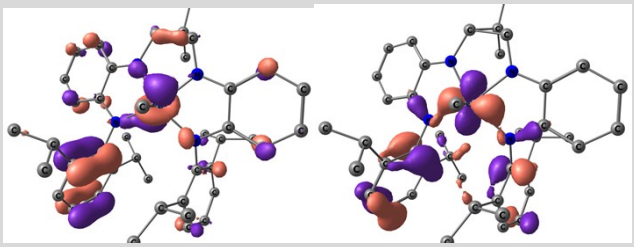

172α; Dipp (π), L (π) 173α; Cr (dδ), L (π)
174α; Dipp (π)

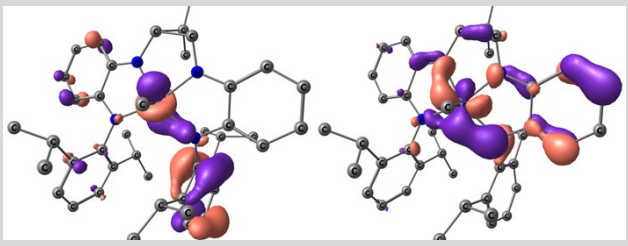

175α; Cr (dσ), Dipp (π) 176α; Cr (d), L (π)

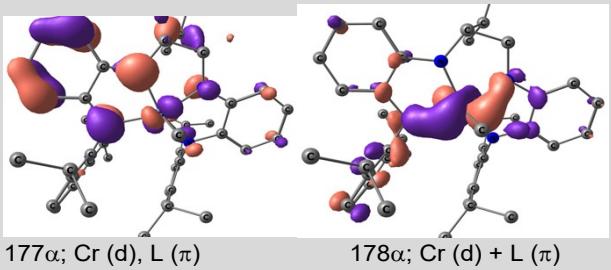

177α; Cr (d), L (π) 178α; Cr (d) + L (π)

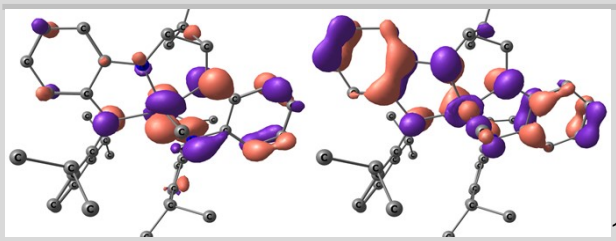

179α; Cr (dπ), L (π) 180α (HOMO); Cr (d), L (π)

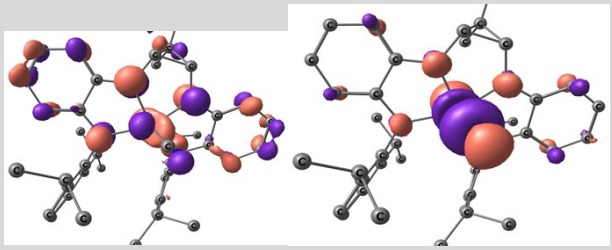

181α (LUMO); Cr (d), L (π*) 182α; CrMe (σ*)

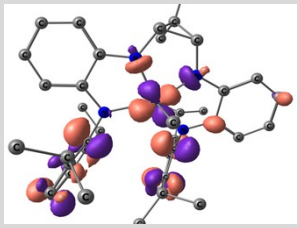

183α; Cr (dδ*), Dipp (π*)

---

ii. **beta orbitals.**

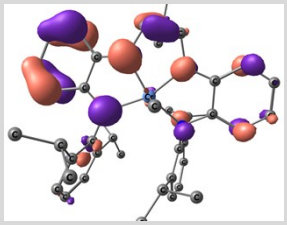

175β; L (π)

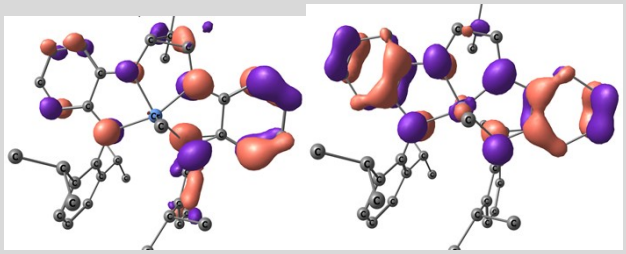

176β; L (π) 177β; L (π)

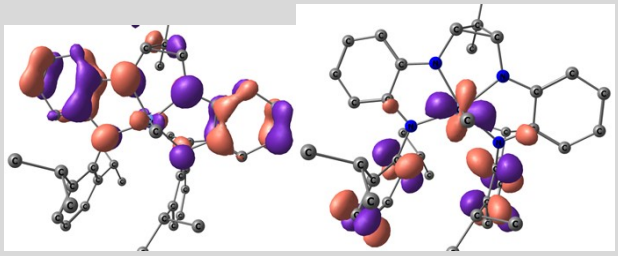

178β (HOMO); L (π) 179β (LUMO); Cr (d), Dipp (π*)

180β; Dipp (π*)
181β; Dipp (π*)
182β; Dipp (π*)

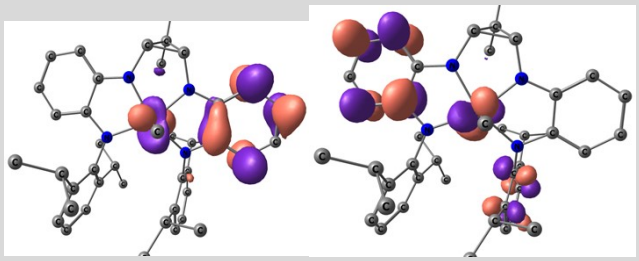

183β; Cr (d), L (π*) 184β; Cr (d), L (π*), Dipp (π*)

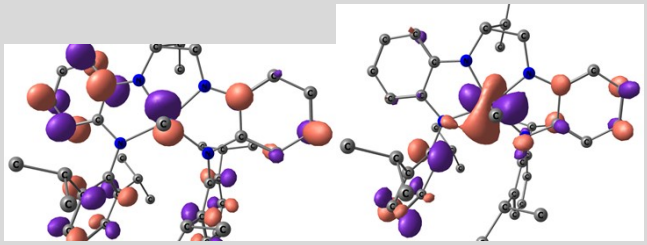

185β; Cr(d), L(π*), Dipp(π*) 186β; Cr(d), L(π*), Dipp (π*)

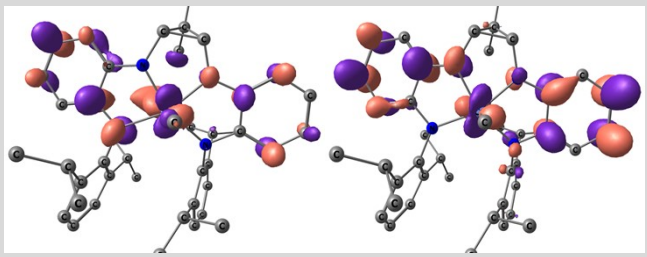

187β; Cr(d), L(π*) 188β; Cr(d), L(π*)

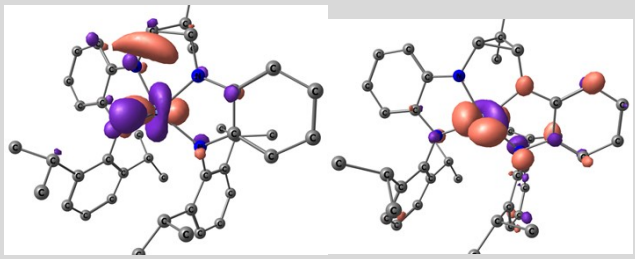

189β; CrMe (σ*), L(π*) 190β; Cr (d), L(π*), CrMe

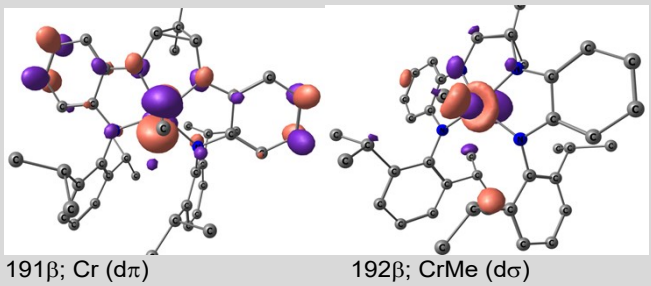

191β; Cr (dπ) 192β; CrMe (dσ)

193β; diffuse
194β; diffuse
195β; diffuse

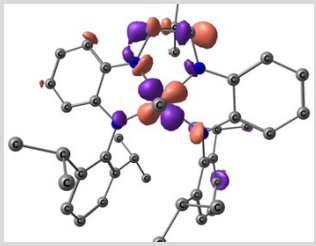

195β; Cr (dδ*)

---

iii. **MO diagram.**

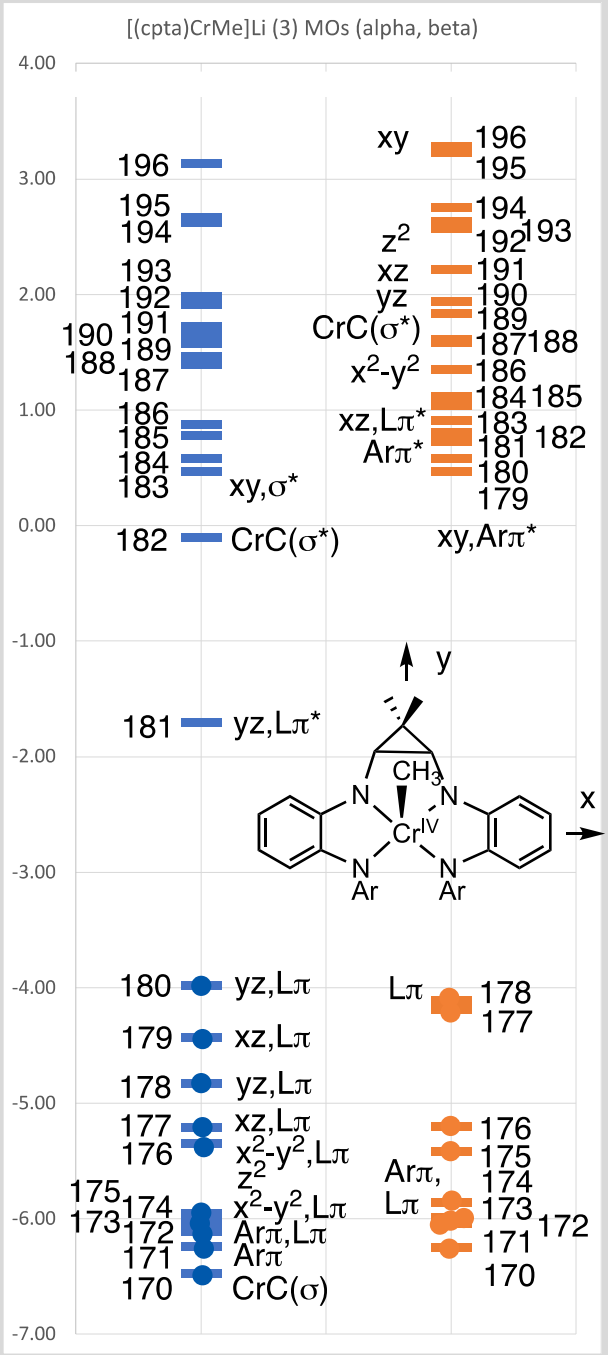

II. References

1 A. A. D'Arpino, T. R. Cundari, P. T. Wolczanski, S. N. MacMillan, *Organometallics* **2023**, *42*, 2747-2761.

2 a) D. F. Evans, *J. Chem. Soc.* **1959**, 2003-2005. b) E. M. Schubert, *J. Chem. Ed.* **1992**, *69*, 62.

3 Frisch, M. J.; Trucks, G. W.; Schlegel, H. B.; Scuseria, G. E.; Robb, M. A.; Cheeseman, J. R.; Scalmani, G.; Barone, V.; Petersson, G. A.; Nakatsuji, H.; Li, X.; Caricato, M.; Marenich, A. V.; Bloino, J.; Janesko, B. G.; Gomperts, R.; Mennucci, B.; Hratchian, H. P.; Ortiz, J. V.; Izmaylov, A. F.; Sonnenberg, J. L.; Williams; Ding, F.; Lipparini, F.; Egidi, F.; Goings, J.; Peng, B.; Petrone, A.; Henderson, T.; Ranasinghe, D.; Zakrzewski, V. G.; Gao, J.; Rega, N.; Zheng, G.; Liang,

W.; Hada, M.; Ehara, M.; Toyota, K.; Fukuda, R.; Hasegawa, J.; Ishida, M.; Nakajima, T.; Honda, Y.; Kitao, O.; Nakai, H.; Vreven, T.; Throssell, K.; Montgomery Jr., J. A.; Peralta, J. E.; Ogliaro, F.; Bearpark, M. J.; Heyd, J. J.; Brothers, E. N.; Kudin, K. N.; Staroverov, V. N.; Keith, T. A.; Kobayashi, R.; Normand, J.; Raghavachari, K.; Rendell, A. P.; Burant, J. C.; Iyengar, S. S.; Tomasi, J.; Cossi, M.; Millam, J. M.; Klene, M.; Adamo, C.; Cammi, R.; Ochterski, J. W.; Martin, R. L.; Morokuma, K.; Farkas, O.; Foresman, J. B.; Fox, D. J. *Gaussian 16 Rev. C.01*, Wallingford, CT, 2016

4 Zhao, Y.; Truhlar, D. G. *Acc. Chem. Res.* **2008**, *41*, 157-167.

5 Cramer, C. J.; Truhlar, D. G., *Phys. Chem. Chem. Phys.* **2009,** *11*, 10757-10816.